

Morphology and environment-dependent fluorescence in blends containing a phenylenevinylene-conjugated polymer

Melissa A. Summers^a, Steven K. Buratto^a, Ludvig Edman^{b,*}

^a Department of Chemistry and Biochemistry, University of California, Santa Barbara, CA 93105, USA

^b Department of Physics, Umeå University, SE-901 87 Umeå, Sweden

Received 5 December 2006; received in revised form 30 March 2007; accepted 5 April 2007

Available online 18 April 2007

Abstract

Near-field scanning optical microscopy and single-molecule spectroscopy have been employed to study a large number of blends containing a highly fluorescent and amorphous conjugated polymer, ‘superyellow’ (a phenylenevinylene copolymer). We find that blend films with a non-fluorescent and semi-crystalline polymer, poly(ethylene oxide) (PEO), with a superyellow content between 9 and 50 mass% exhibit phase separation with no evidence for admixing of the two components, while films with a lower superyellow content of ≤ 1 mass% content comprise a solid-state solution of superyellow within a crystalline PEO matrix. Interestingly, films with approximately the same amount of superyellow as PEO (similar to those used in, e.g., light-emitting electrochemical cells) exhibit a bi-continuous network morphology. We also report that the superyellow fluorescence spectrum shows a remarkable sensitivity to the physical and chemical environment of superyellow.

© 2007 Elsevier B.V. All rights reserved.

Keywords: Near-field scanning optical microscopy; Single-molecule spectroscopy; Poly(*para*-phenylenevinylene); Poly(ethylene oxide); Blends; Morphology; Fluorescence; Bi-continuous network

1. Introduction

The morphology and admixing of multi-component films are important topics in the field of organic electronics, where devices such as photovoltaic cells, light-emitting diodes and light-emitting electrochemical cells (LECs) are often based on films of two or more blended or layered organic phases [1–11]. The morphology of multi-component organic films can be quite complex, due to the interactions of the components with one another and with the substrate and air interfaces. Nominally identical blends of organic polymers can, in addition, result in films with different morphology and varying degrees of phase separation because of differences in the processing conditions [12,13], which are issues of particular relevance for device applications where mobility, domain size and percolation pathways to electrodes are critical features. Scanning-probe microscopy, e.g., atomic force microscopy (AFM), or transmission electron microscopy (TEM) can reveal much about the

detailed morphologies in blend films, but these techniques cannot access the optical properties of chromophores embedded in the film, which is of interest for blends involving fluorescent conjugated polymers. Near-field scanning optical microscopy (NSOM) is well suited to characterize such blends containing conjugated polymers because it provides fluorescence images concurrently with images of sample topography [3,14–16], and because it provides sub-diffraction limited imaging, allowing for optical resolution of ~ 50 nm (approximately the diameter of the optical fiber tip aperture) [17–19].

In this study, we employ a combination of NSOM and single-molecule spectroscopy to explore the nano-scale morphology and fluorescence properties of films comprising a highly fluorescent and amorphous conjugated poly-phenylenevinylene (PPV) polymer, ‘superyellow’ (SY), blended with non-fluorescent polymeric and small molecule organic materials. Notably, we find that spin-cast and annealed blends of SY and poly(ethylene oxide) (PEO) exhibit a concentration dependent morphology: at high SY concentrations (9–50 mass%), complete phase separation with no indications for admixing between the two components takes place; while at lower SY concentration (≤ 1 mass%), a complete

* Corresponding author. Tel.: +46 90 7865732; fax: +46 90 7866673.

E-mail address: ludvig.edman@physics.umu.se (L. Edman).

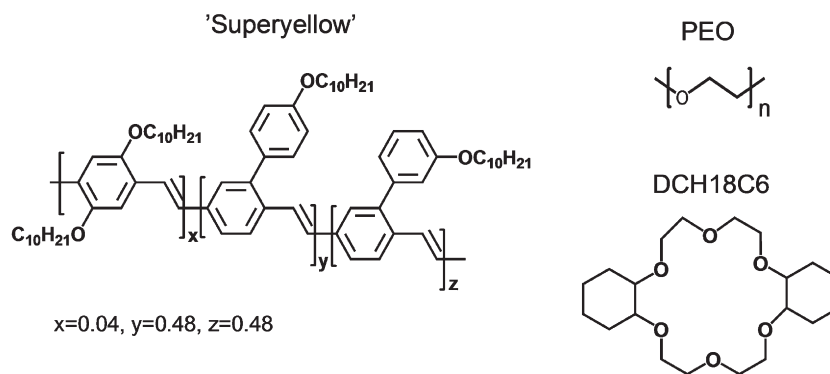


Fig. 1. Molecular structures of the conjugated polymer superyellow, poly(ethylene oxide) (PEO), and the DCH18C6 crown ether.

dissolution of superyellow within a crystalline PEO matrix is apparent. We also find that the photo-physical properties of SY make it a sensitive probe of the chemical and physical properties of the SY environment.

2. Experimental details

SY, which is a commercial polymer engineered specifically for organic electronic applications with a superior amorphous film-forming property, was acquired from Covion and required no additional purification. The other polymers, PEO (Aldrich) and poly(methylmethacrylate) (PMMA, Aldrich), were also used as received, while the *cis*-dicyclohexano-18-crown-6 crown ether (DCH18C6, Acros Organics) was dried at 40 °C under vacuum. See Fig. 1 for molecular structures.

SY/PEO and SY/DCH18C6 films were prepared by spin-coating solutions on carefully cleaned glass coverslips in a glove box using the same methods employed in making films for LEC devices [20,21]. All such blend films were annealed at 70 °C for at least 2 h before testing, which is above the melting transitions of crystalline PEO ($T_m \sim 60$ °C) and crystalline DCH18C6 ($T_m \sim 47\text{--}53$ °C). Care was taken to perform experiments on fresh films. For the PEO-based films, the morphology only changed slightly as the film aged. For the DCH18C6-based films, exposure to air caused a complete dewetting of the film from the surface of the glass substrate within 24 h, possibly due to the hygroscopic nature of the crown ether. For the single-molecule spectroscopy study, a dilute SY solution was dissolved in a 1 mg/mL solution of either PEO or PMMA to yield an average SY lateral spacing of ~ 1 μm in $\sim 50\text{--}100$ nm thick dry films. Neat films of both PEO and PMMA were checked for fluorescence impurities prior to single molecule imaging, to ensure a low-fluorescence background.

NSOM studies were carried out using an Aurora-3 (Veeco Metrology, Santa Barbara, CA) equipped with an EG&G single-photon-counting avalanche photodiode. The 457-nm line of an Ar⁺ laser was used for fluorescence excitation. A Princeton Instruments Spec 10 CCD camera recorded fluorescence spectra. It should be noted, when comparing different NSOM fluorescence intensity images, that the fluorescence counts depend on a number of factors including the diameter of the optical fiber tip aperture, laser-to-fiber coupling efficiency, and

the alignment/efficiency of the collection optics. It is therefore difficult to compare the intensity levels from one image to the next, but the intensity within a given image is on a relative scale. Single-molecule spectroscopy was performed using a custom-built confocal microscope [22,23]. All NSOM and single-molecule spectroscopy experiments were performed in air at room temperature.

3. Results and discussion

3.1. The morphology of mass-balanced SY/DCH18C6 and SY/PEO films

Fig. 2 presents NSOM images of a SY/DCH18C6 film with a mass ratio of 1:1. We find no signs of phase separation in neither the topography (left) nor the fluorescence (right) images, which unambiguously demonstrate that a very intimate mixing between the polymeric SY and the small molecule DCH18C6 takes place. It is, however, relevant to point out that very minor phase separation still can occur in the film, provided it is of a too minor magnitude to be topographically and optically resolved by the NSOM tip. The morphology of a similar blend film with LiCF₃SO₃ salt added has previously been characterized with AFM in tapping mode, and the results demonstrated a very slight phase separation on a length scale of ~ 25 nm [24].

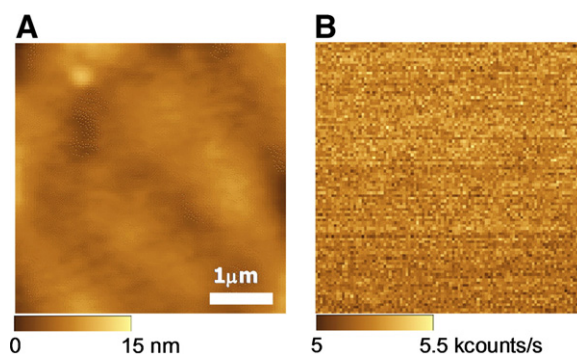


Fig. 2. $5 \mu\text{m} \times 5 \mu\text{m}$ NSOM topography (A) and fluorescence (B) images of a SY/DCH18C6 film with a mass ratio of 1:1.

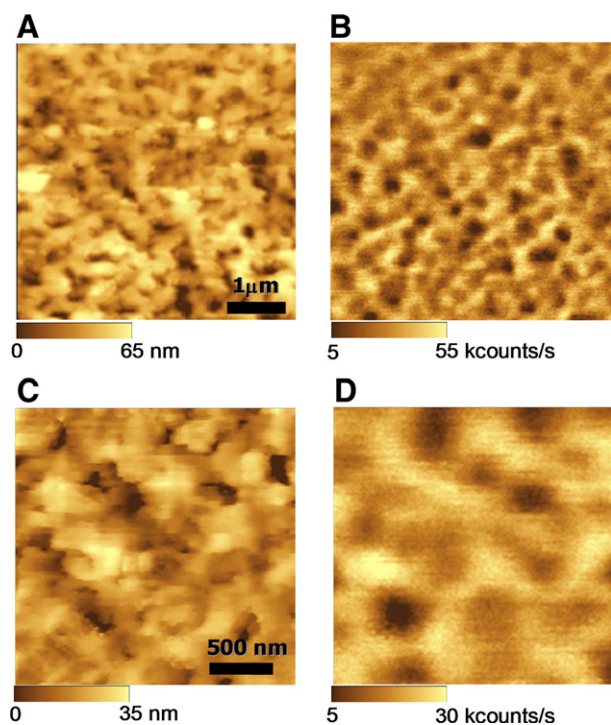


Fig. 3. $5\ \mu\text{m} \times 5\ \mu\text{m}$ NSOM topography (A) and fluorescence (B) images of a SY/PEO film with a mass ratio of 1:1. $2\ \mu\text{m} \times 2\ \mu\text{m}$ NSOM topography (C) and fluorescence (D) images of the same film.

Fig. 3 presents topography (left) and fluorescence (right) NSOM images, with different magnification, of a SY/PEO film with a mass ratio of 1:1. The topography images are comparatively better resolved because the resolution of the shear-force topography is better than the aperture-limited optical resolution. In contrast to the morphology of the SY/DCH18C6 blend films with the same mass ratio (see Fig. 2), we observe a pronounced nano-scale structure in the topography images, and a pattern of dark, dim, and bright regions in the fluorescence images. The smaller scan region in Fig. 3C and D reveals a rough topography and that highly fluorescent SY-rich regions not uniquely correspond to either high or low features in the topography. The latter suggests that neither the SY nor the PEO component has an exclusive tendency to accumulate at the air interface. Nevertheless, both topography and fluorescence NSOM images provide evidence for that SY/PEO films with a mass ratio of 1:1 phase separate into a bi-continuous network.

TEM images of similar blend films comprising a phenylenevinylene-based conjugated polymer and PEO/LiCF₃SO₃, after the PEO/LiCF₃SO₃ portion had been removed by dissolution in water, show that the conjugated polymer forms a network that bears a strong resemblance to the images in Fig. 3 [25]. Although the resolution of a NSOM is inferior to that of a TEM, NSOM offers the advantage of a straightforward (and specific) imaging capability of the conjugated polymer network (due to its fluorescence), without having to physically remove the non-conducting component as is necessary in TEM imaging. In addition, the NSOM shear-force topography image yields information on in what form the non-conducting component is

incorporated into the conjugated polymer network. Finally, the fact that the small molecule DCH18C6, but not the polymeric PEO, readily mixes with the polymeric SY component is a direct manifestation of the well-established entropy-driven phase separation in polymer–polymer blends [26,27].

3.2. The concentration dependence of the morphology of SY/PEO films

SY/PEO films with mass ratios of 10:1, 1:10, 1:100, and 1:1000 were prepared and studied (in addition to the 1:1 film presented in Fig. 3) to allow for a systematic investigation of the effects of SY concentration on film morphology and phase separation. It is further interesting to explore to what extent the two components admix in an apparently phase-separated film, and what the effects of film morphology are on the nano-scale photophysical properties of SY.

Fig. 4 presents topography (left) and fluorescence (right) NSOM images of a SY/PEO film with a mass ratio of 10:1. We find that the morphology is completely dominated by the amorphous SY component, and that the film, accordingly, has a flat topography, with the exception of a few very small (<7 nm) bumps that probably either are minor aggregates of PEO or particle contaminants. The fluorescence image reveals no contrast, suggesting that the non-fluorescent PEO is completely admixed into the fluorescent SY phase or that the PEO domains are much smaller than the $\sim 50\ \text{nm}$ diameter of the aperture of the NSOM tip.

Fig. 5 presents NSOM images of different magnification of a SY/PEO film with a mass ratio of 1:10. The topography images (left) present a structured surface dominated by a crystalline PEO phase, while the fluorescence images (right) reveal a distinct phase separation between the minority-component fluorescent SY phase and the majority-component non-fluorescent PEO phase. The observed topographical structure is consistent with the commonly observed spherulitic morphology of crystalline PEO (as probed in detail by, e.g., TEM [28]), which suggests that the presence of SY at a 9 mass% concentration not interferes significantly with the crystallization of PEO. Importantly, in contrast to the SY/PEO film with a mass ratio of 1:1 (see Fig. 3), the SY clusters at this lower

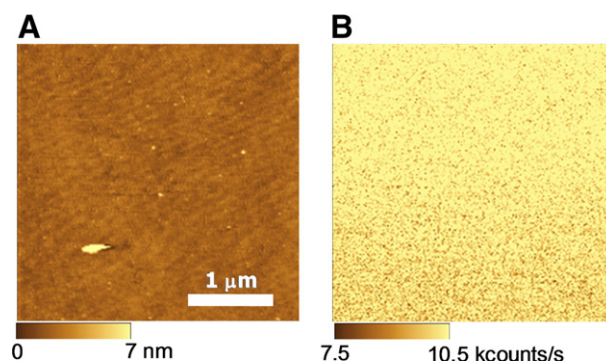


Fig. 4. $4.65\ \mu\text{m} \times 4.65\ \mu\text{m}$ NSOM topography (A) and fluorescence (B) images of a SY/PEO film with a mass ratio of 10:1.

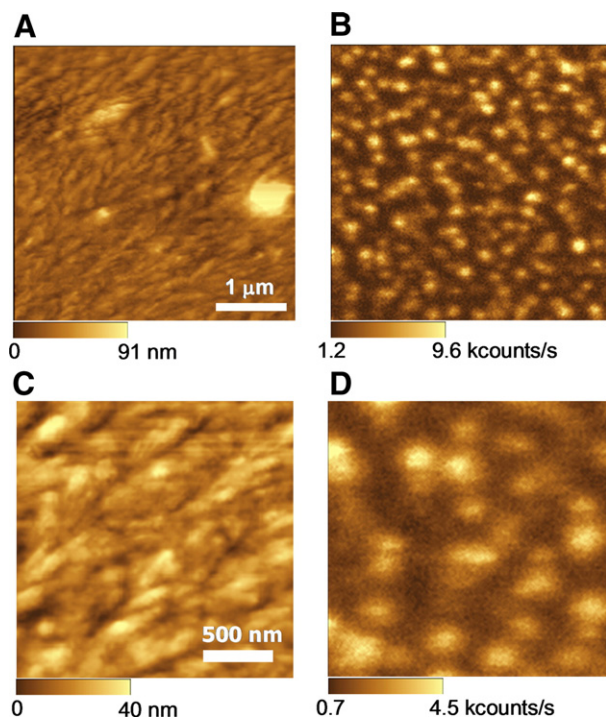


Fig. 5. $5\ \mu\text{m} \times 5\ \mu\text{m}$ NSOM topography (A) and fluorescence (B) images of a SY/PEO film with a mass ratio of 1:10. $2\ \mu\text{m} \times 2\ \mu\text{m}$ NSOM topography (C) and fluorescence (D) images of the same film.

concentration are isolated (the detector counts between SY domains are of the typical background signal level of ~ 1 kcounts/s). Consequently, the threshold SY content for a continuous network formation in a PEO matrix is in the range between 9 and 50 mass%.

Fig. 6 presents NSOM images for SY/PEO films with a mass ratio of 1:100 (top part) and 1:1000 (bottom part), respectively. The topography images (left) are essentially identical to the spherulitic crystalline PEO structure apparent in the 1:10 film (see Fig. 5A and C), while the fluorescence images (right) reveal that an interesting change in the SY morphology has occurred. The isolated and periodic bright SY domains apparent in the film with a SY concentration of 9 mass% (see Fig. 5B and D) are replaced by an essentially uniform fluorescence in these low-SY concentration films. The above results suggest that at low SY concentrations (≤ 1 mass%), the SY molecules are forming a solid-state solution within a crystalline PEO matrix, while at higher SY concentrations (9–50 mass%) a spinodal decomposition process takes place which results in a periodic phase-separated structure. We present further experimental data in favor of this proposed behavior below.

3.3. Nano-scale fluorescence spectroscopy

Fig. 7 presents NSOM nano-scale fluorescence spectra (right) in combination with NSOM fluorescence images (left) for SY/PEO blend films with a mass ratio ranging from 1:1 (top) to 1:1000 (bottom). All fluorescence spectra recorded for the same mass ratio were essentially identical, even though the

intensity of the fluorescence within one such film exhibited a spatial variation in accordance with the results presented in the corresponding fluorescence image to the right. A comparison of the shape and position of the nano-scale fluorescence spectra recorded from the different mass-ratio films reveals a general spectral trend in that the entire spectral envelope and the maximum fluorescence wavelength (λ_{max}) blue-shift with decreasing relative SY content, from $\lambda_{\text{max}} \approx 550$ nm for the SY/PEO film with a 1:1 mass-ratio to $\lambda_{\text{max}} \approx 490$ nm for the 1:1000 film.

More specifically, the nano-scale fluorescence spectra from the 1:1 and, to a slightly lesser extent, the 1:10 film are very similar to that of bulk SY (not shown), which suggests that the emitting SY molecules within the 1:1 and 1:10 films are almost entirely surrounded by other SY molecules. Consequently, in combination with the morphology results presented in the previous section, it appears clear that for a SY concentration range between 9 and 50 mass%, a phase-separated structure exists in which very little admixing between the SY and PEO domains takes place.

For the more SY-dilute 1:100 and 1:1000 films in Fig. 7, the spectral change is dramatic in comparison to the more SY-rich films (and bulk SY), as λ_{max} is significantly blue-shifted and the spectral envelope changes shape to become more narrow with a well resolved vibronic structure for the 1:1000 film. This demonstrates that the environment and/or conformation of the SY molecules in such SY dilute films are distinctly different than in the SY rich films. We find it particularly interesting that

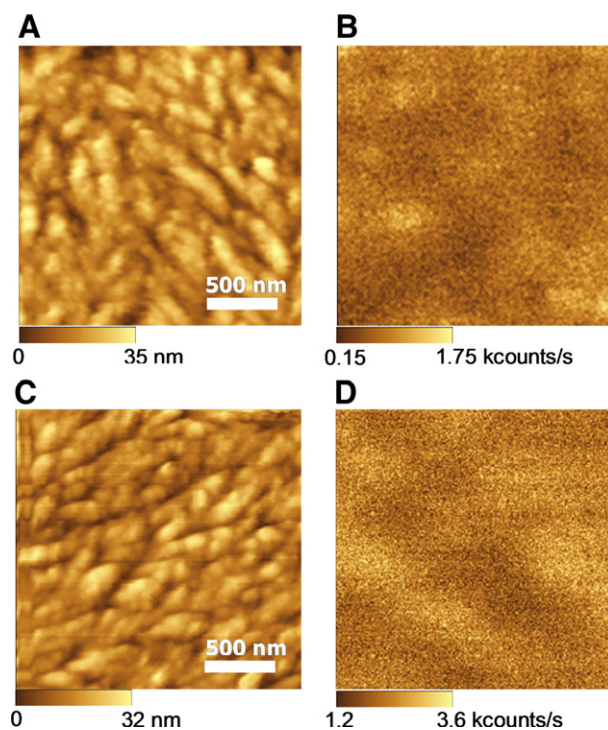


Fig. 6. $2\ \mu\text{m} \times 2\ \mu\text{m}$ NSOM topography (left) and fluorescence (right) images of SY/PEO films with a mass ratio of 1:100 (A and B) and 1:1000 (C and D), respectively.

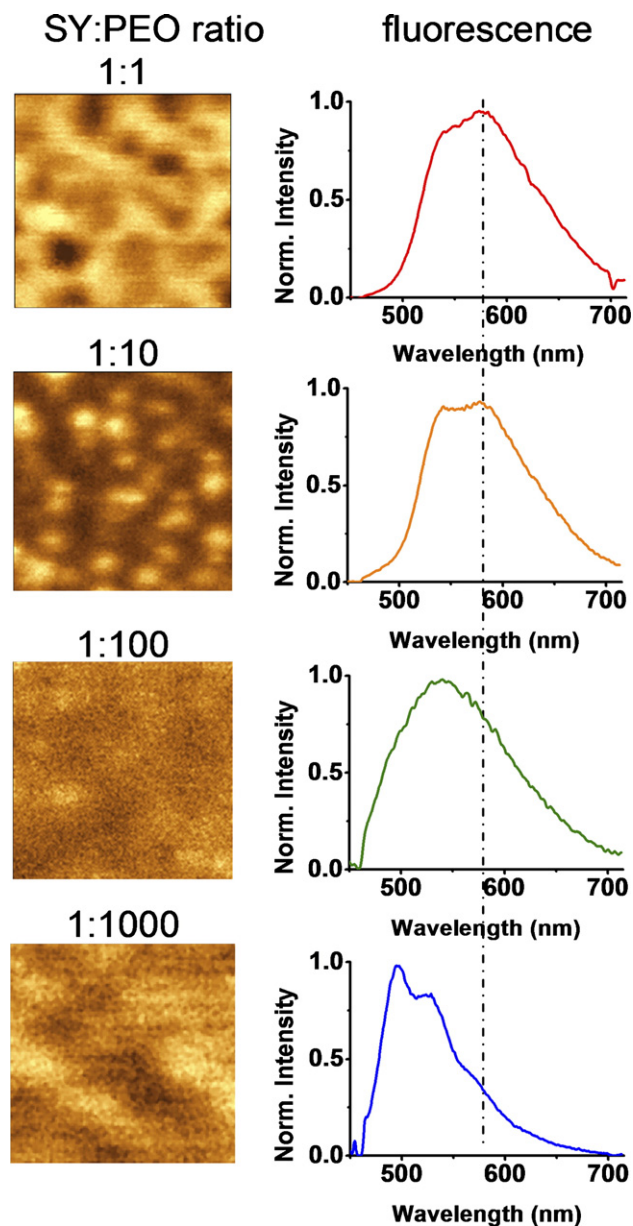


Fig. 7. NSOM nano-scale fluorescence spectra (right) and corresponding 2 μm × 2 μm fluorescence images (left) for SY/PEO blend films with the following mass ratios (from top to bottom): 1:1, 1:10, 1:100 and 1:1000. The dot-dash line indicates the position of λ_{max} for the 1:1 film emission, and is included to illustrate the extent of blue-shifting with decreasing relative SY content.

the onset of this spectral change coincides with the appearance of a distinctly different spatial distribution of the fluorescence, as the spatial origin of the fluorescence changes from large domains for the 1:10 and 1:1 films to become essentially uniform for the 1:100 and 1:1000 films.

3.4. Single-molecule spectroscopy

In order to establish whether the observed blue-shift in the SY fluorescence spectra from SY-dilute SY/PEO films in Fig. 7 is due solely to a decreased intermolecular interaction between isolated

SY molecules (leading to, e.g., decreased excimer-like emission and/or hindered intermolecular diffusion of excitons to low-energy-emitting sites) or whether it also results from an environment-induced change in the conformation of isolated SY molecules, we performed a single-molecule spectroscopy study on SY molecules in different environments. Fig. 8A presents a confocal fluorescence image recorded from a SY/PEO film with a nominal mass ratio of $1:10^6$, in which the average lateral spacing between SY molecules is estimated to be ~1 μm (see experimental section for more details). We postulate that the SY molecules are completely isolated from each other in such extremely dilute films, which is also supported by the emission pattern in Fig. 8A. Fig. 8B presents single-molecule fluorescence spectra recorded from the same SY/PEO film (red, solid) and from a SY/PMMA film with the same extremely dilute SY concentration (blue, dashed). Slight temporal changes were typically observed in the band shape of the fluorescence spectrum from a probed isolated SY molecule (which is in agreement with the widely reported “spectral wandering”

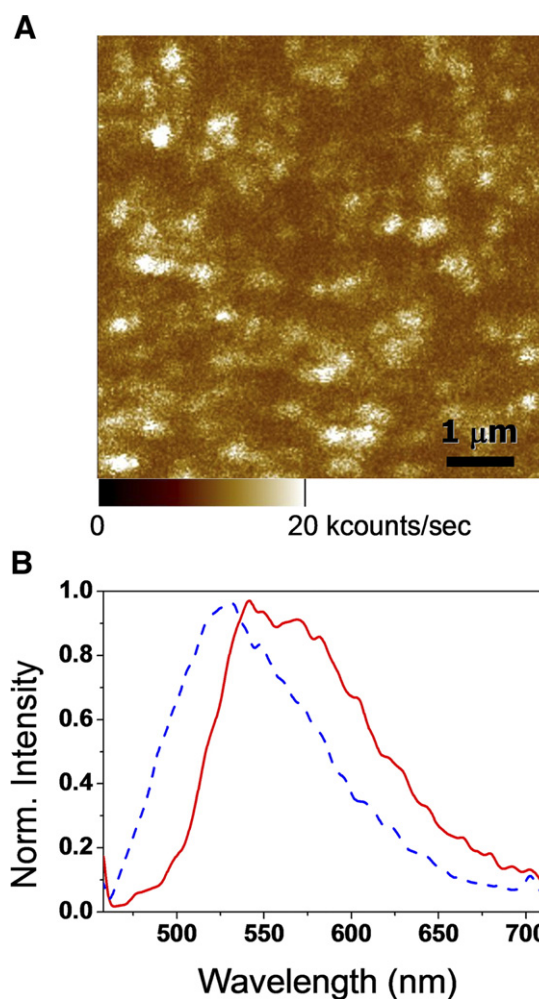


Fig. 8. (A) 9 μm × 9 μm confocal fluorescence image of single SY molecules in a non-annealed PEO matrix. (B) Representative fluorescence spectra obtained from single SY molecules in a non-annealed and rubbery PEO matrix (red, solid) and in a glassy PMMA matrix (blue, dashed), respectively.

phenomenon in similar isolated conjugated polymers [29]), but the results presented in Fig. 8B are representative of the average single-molecule spectrum of SY in each environment.

Here, it is relevant to point out that the above single-molecule films were *not* annealed after the spin-coating process, which accordingly implies that the PEO-based film in Fig. 8 is in a rubbery state (the glass transition temperature, T_g , of amorphous PEO is ~ -50 °C) and that the PMMA-based film is in a glassy state (T_g for PMMA is ~ 80 °C). Consequently, we expect that the SY single molecules in the SY/PEO film are surrounded by a soft rubbery matrix and therefore less restricted than the SY single molecules in the SY/PMMA film that are surrounded by a hard glassy matrix. It is well established that the position and shape of PPV-based conjugated polymer fluorescence spectra are linked to the conformation adopted by the polymer chains, and that conformations leading to shorter persistence lengths yield blue-shifted spectra [30,31]. Thus, it appears reasonable to conclude that the observed marked ~ 30 nm blue-shift of the single-molecule spectrum of SY in going from the PEO-based film to the PMMA-based film in Fig. 8B is related to that the isolated SY molecules are more confined when surrounded by a hard glassy PMMA environment than when surrounded by a soft rubbery PEO environment.

To further investigate the influence of the physical state of the environment on the photo-physical properties of SY, we made a temporal study of the changes in the single-molecule fluorescence spectrum of SY during a controlled transformation of the surrounding PEO matrix from the rubbery state into the crystalline state, via annealing at an elevated temperature (in close proximity to the melting temperature of PEO [32]). Fig. 9 presents representative fluorescence spectra at the following stages of the annealing process: before annealing (dotted green line), after a short-term 5 min annealing at 60 °C (dashed red line), and after a short-term 5 min annealing at 70 °C (solid black line). The observed trends are that the fluorescence spectrum blue-shifts during annealing and that the process is slightly faster at the higher

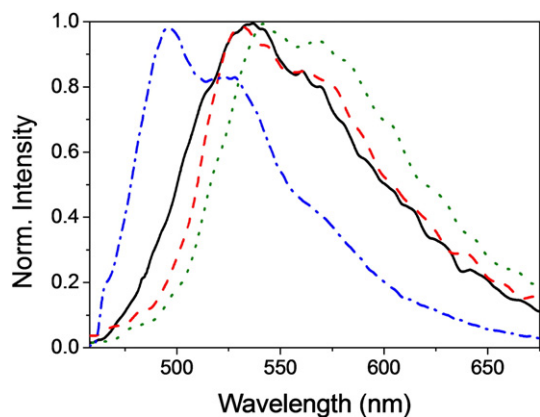


Fig. 9. Single molecule spectra from isolated SY molecules in PEO films that were treated as follows: non-annealed (green, dotted), partially annealed at 60 °C for 5 min (red, dashed), partially annealed at 70 °C for 5 min (black, solid), and completely annealed at 70 °C for 2 h (blue, dot-dashed). Note that the latter spectrum was recorded from a SY:PEO film with a mass ratio of 1:1000.

temperature. This brings further support for the notion that the isolated SY molecules are more confined when positioned in a hard environment (here, partially crystalline PEO) than when positioned in a soft environment (here, rubbery PEO), and that this is manifested in a blue-shifted fluorescence spectrum in harder environments.

The fluorescence spectrum from a SY/PEO film with a mass ratio of 1:1000, which had been annealed at 70 °C for more than 2 h, is also included in Fig. 9 (dot-dashed blue line). The reasons to why the SY fluorescence spectrum from this more SY-concentrated film is more blue-shifted than those originating from the specifically prepared single-molecule films are twofold: (i) annealing at 70 °C for 5 min is not sufficient for a complete rubber–crystalline transformation in such PEO-based films, and (ii) the SY molecules in the 1:1000 film are essentially isolated, and thus forming a solid-state SY solution within the crystalline PEO matrix. These conclusions are further supported by that the fluorescence spectrum from the completely annealed 1:1000 film has a narrower band shape and a more well-resolved vibronic structure, when compared to less crystalline PEO films (see Fig. 9) and more SY-concentrated films (see Fig. 7).

4. Conclusions

We demonstrate that NSOM is a convenient and powerful technique for facile characterization of the morphology and optical properties of conjugated polymer-containing blends. Specifically, we find that annealed spin-cast blend films between the conjugated polymer SY and PEO exhibit a concentration-dependent morphology and phase mixing: at high SY concentrations (>90 mass%) the film morphology is completely dominated by the amorphous SY, at low SY concentrations (<1 mass%) the film morphology comprises a solid-state solution of SY molecules within a crystalline PEO matrix, while at intermediate SY concentrations (9–50 mass%) a phase-separated structure with no admixing of the two components is apparent. By employing single-molecule spectroscopy, we also demonstrate that the photo-physical properties of isolated SY molecules are highly sensitive to the environment of SY, and that the fluorescence spectrum of SY blue-shifts when the environment shifts from a soft rubbery PEO to a hard PEO crystal or a hard PMMA glass.

Acknowledgments

The authors wish to thank Prof. Alan J. Heeger and Prof. Rachel Segalman for valuable insight and discussion. Dr. Stephan Kämmer, Richard Puestow and Veeco Metrology are gratefully acknowledged for their expertise in NSOM imaging and spectroscopy and for loan of an Aurora III NSOM. L.E. is grateful for generous support from the Wenner-Gren foundations.

References

- [1] D. Richards, F. Cacialli, Philos. Trans. R. Soc. Lond., A 362 (2004) 771.
- [2] C.H. Yang, Q.J. Sun, J. Qiao, Y.F. Li, J. Phys. Chem., B 107 (2003) 12981.

- [3] A.C. Morteani, A.S. Dhoot, J.S. Kim, C. Silva, N.C. Greenham, C. Murphy, E. Moons, S. Cina, J.H. Burroughes, R.H. Friend, *Adv. Mater.* 15 (2003) 1708.
- [4] S. Tasch, E.J.W. List, O. Ekstrom, W. Graupner, G. Leising, P. Schlichting, U. Rohr, Y. Geerts, U. Scherf, K. Mullen, *Appl. Phys. Lett.* 71 (1997) 2883.
- [5] G. Wegmann, B. Schweitzer, M. Hopmeier, M. Oestreich, H. Giessen, R.F. Mahrt, *Phys. Chem. Chem. Phys.* 1 (1999) 1795.
- [6] L. Ding, M. Jonforsen, L.S. Roman, M.R. Andersson, O. Inganäs, *Synth. Met.* 110 (2000) 133.
- [7] L. Edman, *Electrochim. Acta* 50 (2005) 3878.
- [8] J.-H. Shin, A. Dzwilewski, A. Iwasiewicz, S. Xiao, Å. Fransson, G.N. Anka, L. Edman, *Appl. Phys. Lett.* 89 (2006) 013509.
- [9] R.A. Segalman, *Mater. Sci. Eng., R Rep.* 48 (2005) 191.
- [10] J. Gao, G. Yu, A.J. Heeger, *Appl. Phys. Lett.* 71 (1997) 1293.
- [11] F.P. Wenzl, P. Pachler, C. Suess, A. Haase, E.J.W. List, P. Poelt, D. Somitsch, P. Knoll, U. Scherf, G. Leising, *Adv. Funct. Mater.* 14 (2004) 441.
- [12] W.K. Kim, K. Char, C.K. Kim, *J. Polym. Sci., Polym. Phys. Ed.* 38 (2000) 3042.
- [13] J. Heier, E.J. Kramer, P. Revesz, G. Battistig, F.S. Bates, *Macromolecules* 32 (1999) 3758.
- [14] J. Teetsov, D.A. Vanden Bout, *J. Phys. Chem., B* 104 (2000) 9378.
- [15] J. Teetsov, D.A. Vanden Bout, *Macromol. Symp.* 167 (2001) 153.
- [16] J. Chappell, D.G. Lidzey, *J. Microsc. (Oxford)* 209 (2003) 188.
- [17] E. Betzig, J.K. Trautman, T.D. Harris, J.S. Weiner, R.L. Kostelak, *Science* 251 (1991) 1468.
- [18] R.C. Dunn, *Chem. Rev.* 99 (1999) 2891.
- [19] S.K. Buratto, *Curr. Opin. Solid State Mater. Sci.* 1 (1996) 485.
- [20] L. Edman, D. Moses, A.J. Heeger, *Synth. Met.* 138 (2003) 441.
- [21] L. Edman, M.A. Summers, S.K. Buratto, A.J. Heeger, *Phys. Rev., B* 70 (2004) 115212.
- [22] K.D. Weston, S.K. Buratto, *J. Phys. Chem., A* 102 (1998) 3635.
- [23] M.A. Summers, P.R. Kemper, J.E. Bushnell, M.R. Robinson, G.C. Bazan, M.T. Bowers, S.K. Buratto, *J. Am. Chem. Soc.* 125 (2003) 5199.
- [24] L. Edman, M. Pauchard, D. Moses, A.J. Heeger, *J. Appl. Phys.* 95 (2004) 4357.
- [25] Y. Cao, G. Yu, A.J. Heeger, C.Y. Yang, *Appl. Phys. Lett.* 68 (1996) 3218.
- [26] J. Chappell, D.G. Lidzey, P.C. Jukes, A.M. Higgins, R.L. Thompson, S. O'Connor, I. Grizzi, R. Fletcher, J. O'Brien, M. Geoghegan, R.A.L. Jones, *Nat. Matters* 2 (2003) 616.
- [27] E. Moons, *J. Phys.: Condens. Matter* 14 (2002) 12235.
- [28] S.Z.D. Cheng, J.S. Barley, E.D. Vonmeerwall, *J. Polym. Sci., Polym. Phys. Ed.* 29 (1991) 515.
- [29] D.H. Hu, J. Yu, P.F. Barbara, *J. Am. Chem. Soc.* 121 (1999) 6936.
- [30] M. Kemerink, J.K.J. van Duren, A. van Breemen, J. Wildeman, M.M. Wienk, P.W.M. Blom, H.F.M. Schoo, R.A.J. Janssen, *Macromolecules* 38 (2005) 7784.
- [31] C.L. Gettinger, A.J. Heeger, J.M. Drake, D.J. Pine, *J. Chem. Phys.* 101 (1994) 1673.
- [32] L. Edman, A. Ferry, M.M. Doeff, *J. Mater. Res.* 15 (2000) 1950.